Applied Physics A (2021) 127:297
https://doi.org/10.1007/s00339-021-04451-7

Applied Physics A
Materials Science & Processing

Study on the relaxation mechanism of residual stress in SiCp/6061Al composites based on the surface modification of reinforcement

Zhiqiang Zhu[1] · Qingping Wang[1] · Pakeeza Maryum[1] · Yuxin Liu[1] · Chunyang Lu[1] · Tingting Xue[1] · Biao Hu[1] · Chao Zhang[1] · Ruxiang Qin[2]

Received: 21 December 2020 / Accepted: 19 March 2021 / Published online: 30 March 2021
© The Author(s), under exclusive licence to Springer-Verlag GmbH, DE part of Springer Nature 2021

Abstract

The effect of reinforcement surface modification on the residual stress (RS) in 35vo l%SiCp/6061Al composites was studied, and the experimental conclusions were verified by finite element analysis. The results show that after the SiC particles were modified by pickling, ultrasonic stirring and high-temperature oxidation (1100 ℃/6 h), the composite has the lowest RS, which was only 1.1 MPa. Microstructure and phase composition of 35vo l%SiCp/6061Al composites have been examined by Scanning Electron Microscope (SEM) and X-Ray Diffraction (XRD). It was found that the reinforcement surface modification was beneficial to promote the improvement of interface bonding state, and the diffraction peaks of Si element have been significantly enhanced. Additionally, the formed Al-Si-SiC interphase has a higher interface adhesion work, which effectively reduced the concentration degree of RS. An interface-phase model based on the surface morphology of real SiC particles was established. The simulation results show that the RS was mainly concentrated in the sharp corners of reinforcement, and the stress level is relatively high. When the sharp corners were eliminated, the stress level gradually decreases. When the Al-Si-SiC interphase was formed, the stress level in SiCp/6061Al composites decreases significantly. The results of finite element simulation and experimental measurement were relatively consistent.

Keywords SiCp/6061Al composites · Residual stress · Surface modification · Finite element analysis

1 Introduction

Particle-reinforced metal-matrix composites (PRMMCs), especially aluminum matrix composites, have been widely used in aerospace and other industries as structural materials [1–3]. However, PRMMCs are prone to generate RS during the high-temperature preparation process and are highly concentrated on the interface region, which brings great obstacles to the significant improvement on the mechanical properties of PRMMCs [4, 5]. Therefore, how to effectively release the RS in PRMMCs has become a key problem that needs to be solved urgently. According to the current research background, related researchers mainly prefer to use heat treatment process optimization technology to release the RS in PRMMCs. Qu SG et al. [6] studied the effect of heat treatment on stress relief of high volume fraction SiCp/Al composites. The results show that the composite which experienced the three-step solution-quenching and aging and 12 times thermal-cold cycling treatments, presented the optimum RS relief effect. Kong KJ et al. [7] studied the relaxation effect of continuous diode laser heating on the RS in 45% SiCp/Al composites and proposed the mechanism of the evolution of dislocation density and dislocation structure arrangements on the relaxation of RS. Obviously, the heat treatment process optimization technology has a certain effect on release the RS in PRMMCs, but there are also a series of problems such as lengthy cycle, complex process and high cost.

Generally speaking, the performance of PRMMCs mainly depends on the microstructure and chemical composition of the selected matrix, reinforcement and interphase [8]. For a given matrix and reinforcement system, the microstructure and chemical composition of interphase are the decisive factors affecting the performance

✉ Qingping Wang
wqp.507@163.com

[1] School of Materials Science and Engineering, Anhui University of Science and Technology, Huainan 232001, China

[2] School of Energy and Security, Anhui University of Science and Technology, Huainan 232001, China

of PRMMCs. Therefore, researchers have been hoped to obtain the desired composite material properties through controlling of interphase precisely [9–11]. The surface modification of reinforcement is an important way to control the interphase of PRMMCs. It plays an important role in improving the wettability of interphase, inhibiting the mutual diffusion between the reinforcement and matrix and slowing down the rate of chemical reaction [12–14]. As a result, more and more researchers have regarded the surface pretreatment of reinforcement as an important research direction. Ni ZL et al. [15] studied the effect of surface modification of SiC particles on the tensile strength and thermal expansion coefficient of SiCp/Al-30Si composites. The results confirmed that the particle surface modification has a significant effect on enhancing the interface bonding strength and improving the mechanical properties. Park J et al. [16] used electroless plating method to make SiO_2, Ni and Si coatings on the surface of SiC particles, and thoroughly discussed the mechanism of surface modification on the wettability and interface bonding state of SiCp/7075Al composites.

Although the current research on the reinforcement surface modification is continuously deepening [17–21], few literatures mention its influence on the RS in PRMMCs, and the research on the reinforcement surface modification on the relaxation mechanism of RS in PRMMCs is particularly scarce[22, 23]. In addition, the blocking effect of interphase in the ideal state can also reduce the concentration degree of RS [24]. Therefore, it is feasible to use the technology of precise control interphase to release the RS in PRMMCs effectively. In this paper, a combination of experimental analysis and numerical simulation was used to preliminarily explore the effect of SiC particles surface modification on the RS in 35vo l%SiCp/6061Al composites, the microstructure and phase composition of SiCp/6061Al composites under different surface modification methods were analyzed, and the relaxation mechanism of SiC particle surface modification on the RS was revealed. It provides theoretical basis and technical guidance for release RS in PRMMCs and expanding its application in most advanced fields.

2 Experimental procedure

2.1 Surface modification of SiC particles

In this paper, 35vo l%SiCp/6061Al composites were prepared by powder metallurgy, and SiC particles with an average particle size of 16 μm were used as the reinforcement. Generally speaking, the pickling agents usually used for SiC particles were mainly dilute hydrochloric acid and washing hydrofluoric acid. Both have the same effect on SiC particles, but dilute hydrofluoric acid will react with SiC particles during the pickling process. (the chemical equation is shown in (1)), resulting in the mass loss of SiC particles. Therefore, dilute hydrochloric acid was used to pickle the surface of SiC particles.

$$SiC(s) + 4HF(l) = SiF_4(g) + CH_4(g) \quad (1)$$

The formulated surface modification process was as follows. Firstly, the pre-weighed SiC particles were added to the dilute hydrochloric acid with a mass fraction of 10%, and the glass rod was used for full stirring until the impurities on the surface of SiC particles were completely removed. Secondly, the acid-washed SiC particles were placed in deionized water and ultrasonically treated with an ultrasonic cleaner and used a glass rod to stir repeatedly. The ultrasonic process parameters mainly include: ultrasonic time of 30 min, ultrasonic temperature of 25 ℃, ultrasonic power of 180 W and standing time of 60 min. Finally, SiC particles after ultrasonic cleaning were fully dried, laid flat on the corundum crucible plate, and calcined to 1100 °C in a muffle furnace and kept for several hours to promoted the SiC particles to be fully oxidized in a high-temperature environment. The experimental parameters of different surface modification methods are shown in Table 1.

2.2 Determination of residual stress

The Proto LXRD micro-zone stress meter was used to measure the RS in 35vo l%SiCp/6061Al composites. In this measurement process, the measurement conditions set as shown in Table 2.

Table 1 Experimental parameters of different surface modification methods

Material code	Volume fraction (%)	Sintering system	Surface modification methods
SiC particles A	35	700℃/2 h	–
SiC particles B	35	700℃/2 h	Pickling + ultrasonic stirring
SiC particles C	35	700℃/2 h	Pickling + ultrasonic stirring + high-temperature oxidation(1100 ℃/2 h)
SiC particles D	35	700℃/2 h	Pickling + ultrasonic stirring + high-temperature oxidation(1100 ℃/4 h)
SiC particles E	35	700℃/2 h	Pickling + ultrasonic stirring + high-temperature oxidation(1100 ℃/6 h)

Table 2 Measurement conditions of X-ray diffraction for the experimental sample

X-ray diffraction items	Measurement conditions
Characteristic X-ray	Cr-Kα
Tube voltage and current	35kv, 35 mA
Diffraction geometry	Side inclination and fixed ψ methods
Diffraction crystal plane	Aluminum alloy (311)
Diffraction angle	139°
Diffraction wavelength	λ = 0.2291 nm
Incident angle Ψ	0.00°, 22.69°, 33.04°, 41.00°, 50.50°
Elastic modulus	70.6GPa
Poisson's ratio	0.34

The RS σ_ψ was calculated from the expression [25]:

$$\sigma_\psi = KM \tag{2}$$

Choose the X-ray with λ = 0.2291 nm and irradiate it on the surface of experimental sample multiple times at different incident angles, measure the corresponding diffraction angle 2θ, and solve the slope M of the 2θ-sin^{2}ψ curve. and M was given by [25]:

$$M = \frac{\partial(2\theta)}{\partial(\mathrm{Sin}^2\psi)} \tag{3}$$

K represents the stress coefficient, which was generally only related to the property of material and the selected diffraction crystal plane. Its calculation equation was [25]:

$$K = -\frac{E}{1+v} Cot\theta_0 \frac{\pi}{360} \tag{4}$$

Here *E* and *v*, respectively, represent the elastic modulus and Poisson's ratio of experimental samples, and θ_0 represents the Bragg angle of the diffraction peak.

3 Results and discussion

3.1 Reinforcement microstructure and phase composition analysis

The microstructure and phase composition of SiC particles with different surface modification methods are shown in Fig. 1.

It can be seen from the SEM images that SiC particles with different modification methods have different surface morphologies. In Fig. 1a, the surface morphology of SiC particles A is extremely irregular on the whole, and most of the SiC particles have sharp corners. In Fig. 1b, the SiC particles B is generally smooth and clean, and the particle size is relatively uniform. There are reasons as follow: on the one hand, the diluted hydrochloric acid can dissolve and remove various impurities attached to the surface of SiC particles. On the other hand, the sharp corners of some SiC particles can be eliminated during the ultrasonic stirring process. In Fig. 1c, the surface of SiC particles E is obviously passivated, which is caused by the formation of a thin film on the surface of SiC particles in a high-temperature environment. In Fig. 1d, XRD analysis shows that the thin film is a SiO_2 layer.

3.2 Analysis of microstructure in 35vol %SiCp/6061Al composites

Based on the results of the above experimental data analysis, the reinforcement surface modification can effectively release the RS in the experimental sample. In order to further study the relaxation mechanism of reinforcement surface modification on the RS in 35vo l%SiCp/6061Al composites, this paper analyzed the microstructure and chemical composition of experimental samples under different surface modification methods.

Figure 2 shows the SEM images of SiCp/6061Al composites prepared under different reinforcement surface modification methods. In Fig. 2a, the SiC particles without surface modification, a large number of new phases appeared on the surface of experimental sample, which is caused by the erosion of SiC particles by molten aluminum alloy and the excessive occurrence of interfacial reactions. There is no doubt that excessive interfacial reactions cause more RS in the experimental samples. Meanwhile, the interface bonding state between SiC particles and aluminum alloy is also relatively poor, resulting in the formation of interphase that cannot effectively transfer the RS, and the SiC particles also appear partial cracks due to the high concentration of RS. In Fig. 2b, the SiC particles have undergone pickling, ultrasonic stirring and high-temperature oxidation (1100 ℃/6 h). The surface of experimental samples is cleaner, and the distribution of SiC particles is more uniform, which indicating that only slight interfacial reactions occurred during the preparation of 35vo l%SiCp/6061Al composites. Moreover, the SiC particles are tightly bonded to the aluminum alloy, which helps to transfer the RS in the reinforcement to matrix.

3.3 Analysis of phase composition in 35vol %SiCp/6061Al composites

Figure 3 shows the phase analysis of 35vo l%SiCp/6061Al composites under different surface modification methods. It can be clearly seen that Al_4C_3, a brittle compound, is not detected in the experimental samples prepared by powder metallurgy. Meanwhile, compared with the SiC particles

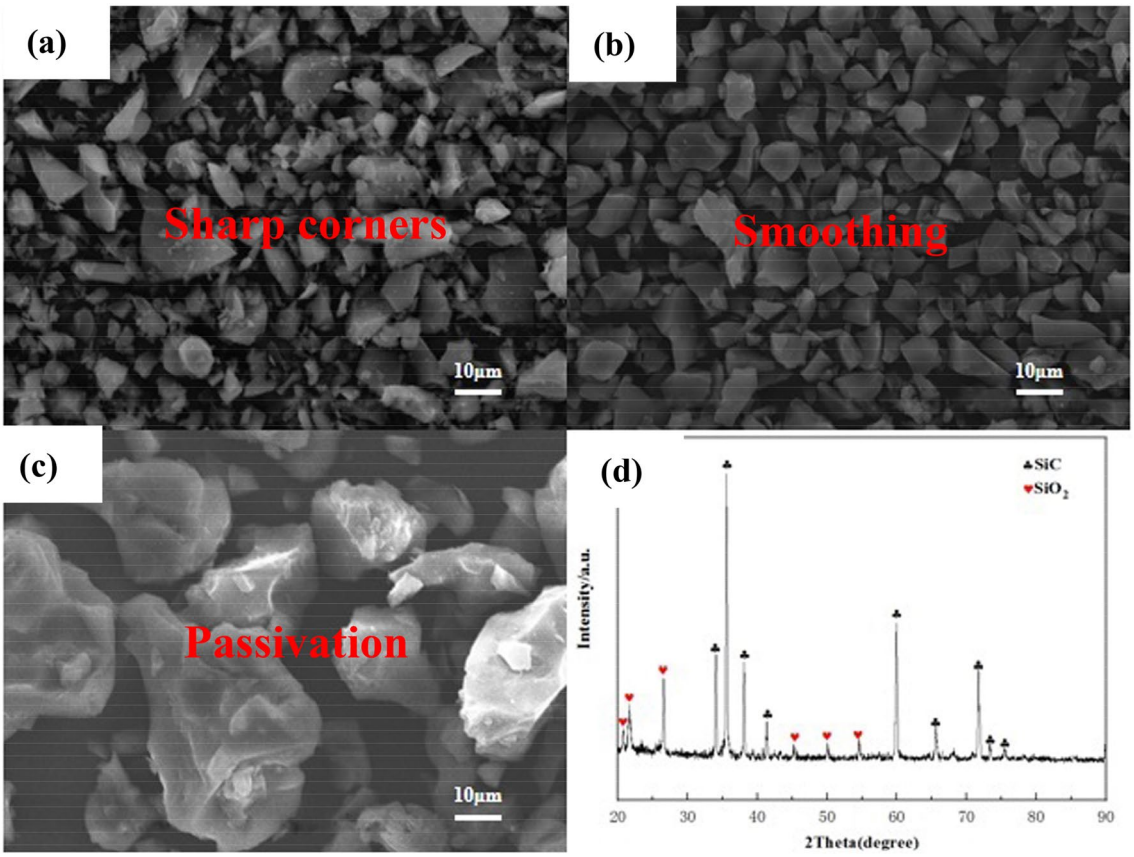

Fig. 1 Microstructure and phase composition of reinforcement: **a** SiC particles A; **b** SiC particles B; **c** SiC particles E; **d** XRD analysis of SiC particles E

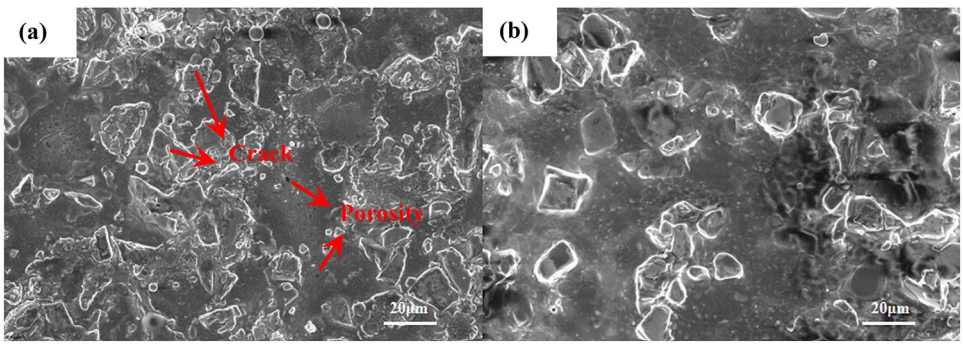

Fig. 2 SEM images of 35vol %SiCp/6061Al composites: **a** SiC particles A; **b** SiC particles E

(A), in the XRD pattern of experimental sample prepared by SiC particles (E), the diffraction peak intensity of Si element is significantly higher. This is because the SiO_2 layer on the surface of SiC particles preferentially comes into contact with the molten aluminum alloy, and a chemical reaction occurs quickly (chemical equations are shown in Eq. 5 and Eq. 6), which eventually leads to the formation of Si element enrichment in the interface region of SiCp/6061Al composites.

$$3SiO_2(s) + 4Al(l) = 2Al_2O_3(s) + 3Si(s) \quad (5)$$

$$2SiO_2(s) + Mg(l) + 2Al(l) = MgAl_2O_4(s) + Si(s) \quad (6)$$

From the chemical equation, compounds such as $MgAl_2O_4$ and Al_2O_3 are also formed in the experimental samples, but Al_2O_3 is replaced by the Mg element in the aluminum alloy during the reaction, so it is only used as

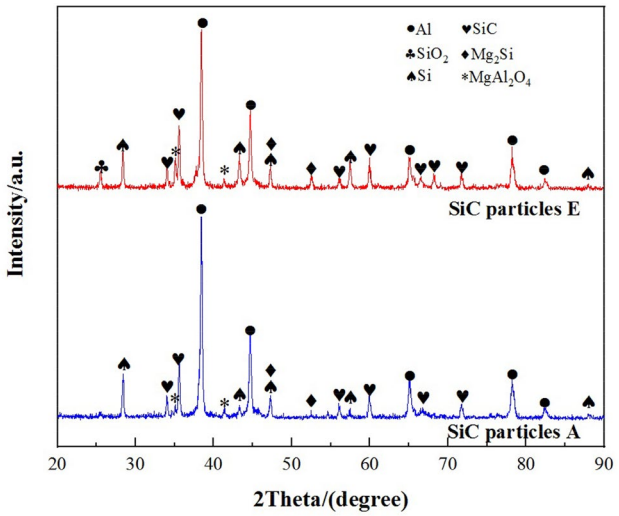

Fig. 3 XRD patterns of 35vo 1%SiCp/6061Al composites under different surface modification methods

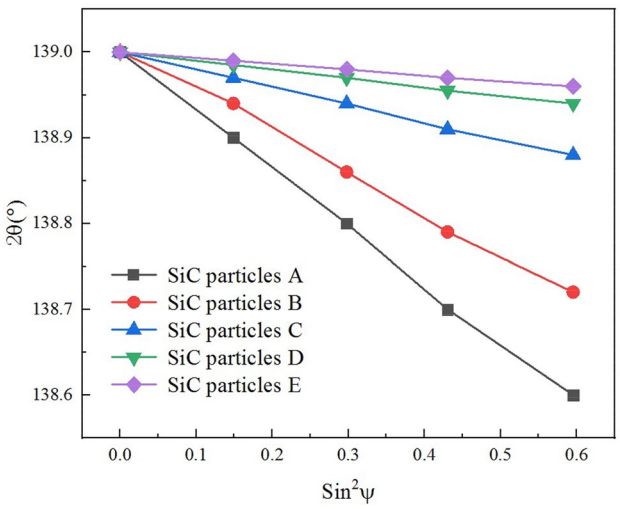

Fig. 4 The relationship between 2θ and $\sin^2\psi$

an intermediate product. Moreover, the diffraction peaks of SiO_2 are detected in the experimental samples that had undergone pickling, ultrasonic stirring and high-temperature oxidation (1100 ℃/6 h), which indicated that some SiO_2 do not participate in the chemical reaction.

3.4 Residual stress analysis

Proto LXRD micro-zone stress meter has some limitations in measuring RS, that is, the selected diffraction Angle 2θ must exceed 130°. Prior to calculate RS of the experimental samples, it is necessary to clarify the slope M of the 2θ-$\sin^2\psi$ curve. In this measurement process, the selected diffraction crystal planes are all aluminum alloys (3 1 1), so a set of incident angles ψ (0.00°, 22.69°, 33.04°, 41.00°, 50.50°) can be selected to determine the corresponding $\sin^2\psi$(0.0000, 0.1489, 0.2977, 0.4304, 0.5954). The constructed 2θ-$\sin^2\psi$ curve is shown in Fig. 2.

Figure 4 shows the 2θ-$\sin^2\psi$ curves of each experimental sample under different surface modification methods. Obviously, the diffraction angle 2θ and $\sin^2\psi$ show a good linear relationship, and with the gradual increase of $\sin^2\psi$, each curve shows a different degree of downward trend. Compared with SiC particles A and SiC particles B, the slope M of SiC particles C, SiC particles D and SiC particles E is relatively low. Combining Eq. (2), the experimental samples corresponding to SiC particles C, SiC particles D and SiC particles E should have smaller RS under theoretical calculation conditions.

In Fig. 5, according to the measurement results, the experimental samples without surface modification have the highest RS, reaching 27.7 MPa. After surface modification with pickling, ultrasonic stirring and high-temperature oxidation, the RS in the experimental samples decreased significantly. In addition, with the extension of the high-temperature oxidation time, the surface of SiC particles is more fully oxidized, the thickness of SiO_2 layer increases relatively, and the RS in the experimental samples also shows a gradually decreasing trend. However, when the high-temperature oxidation time exceeds 4 h, the decline range of RS gradually moderates, which shows that the effect of further extending the high-temperature oxidation time on the RS is relatively small. For SiC particles E, the experimental samples have the lowest RS, which is only 1.1 MPa.

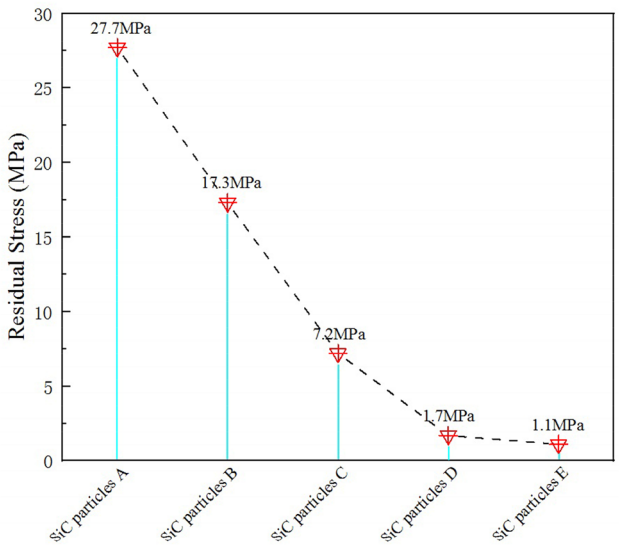

Fig. 5 RS measurement results

3.5 Finite element analysis

3.5.1 Construction of interface-phase model

Combined with the SEM image of Fig. 1, the surface morphology of SiC particles has changed significantly under different surface modification methods. In order to further study the effect of SiC particles surface morphology on the RS in SiCp/6061Al composites, an interface-phase model based on the real surface morphology of SiC particle was constructed in this paper. The interface-phase model constructed by ABAQUS finite element software is shown in Fig. 6.

In Fig. 6a, the SiC particles have not undergone surface modification, the reinforcement in the interface-phase model has sharp corners, and the reinforcement and matrix are in contact with each other, which easily leads to excessive erosion of reinforcement. In Fig. 6b, the SiC particles have undergone pickling and ultrasonic stirring, the sharp corners of reinforcement in the interface-phase model are broken, but the contact between the reinforcement and matrix is still maintained. After high-temperature oxidation, a SiO_2 layer was formed on the surface of reinforcement, and an Al-Si-SiC interphase was formed through a chemical reaction. As the high-temperature oxidation time increases, the thickness of Al-Si-SiC interphase is also gradually increase, the established interface-phase model is shown in Fig. 6c, d and e.

In the process of finite element calculation of RS, the physical properties involved in matrix, reinforcement and interphase mainly include density, thermal conductivity, specific heat, elastic modulus, Poisson's ratio and thermal expansion coefficient. The values and units of physical properties of each component of SiCp/6061Al composites are summarized in Table 3.

3.5.2 Setting of boundary conditions

During the high-temperature cooling process of SiCp/6061Al composites, a large amount of RS was generated. In order to ensure that the interface-phase model real reflected the changes in the level and distribution of RS, in the simulation process, the temperature load conditions were applied, and the temperature was reduced from 700 ℃ to 20 ℃. The interface-phase model was prone to rigid displacement during temperature load, which makes it unable to be solved by the finite element analysis method [28, 29]. Therefore, it was necessary to constrain the interface-phase model by imposing boundary conditions. In the interface-phase model, the horizontal and vertical displacement changes of the Y-axis and X-axis were, respectively, set to zero, that was U1 = UR2 = UR3 = 0, U2 = UR1 = UR3 = 0,

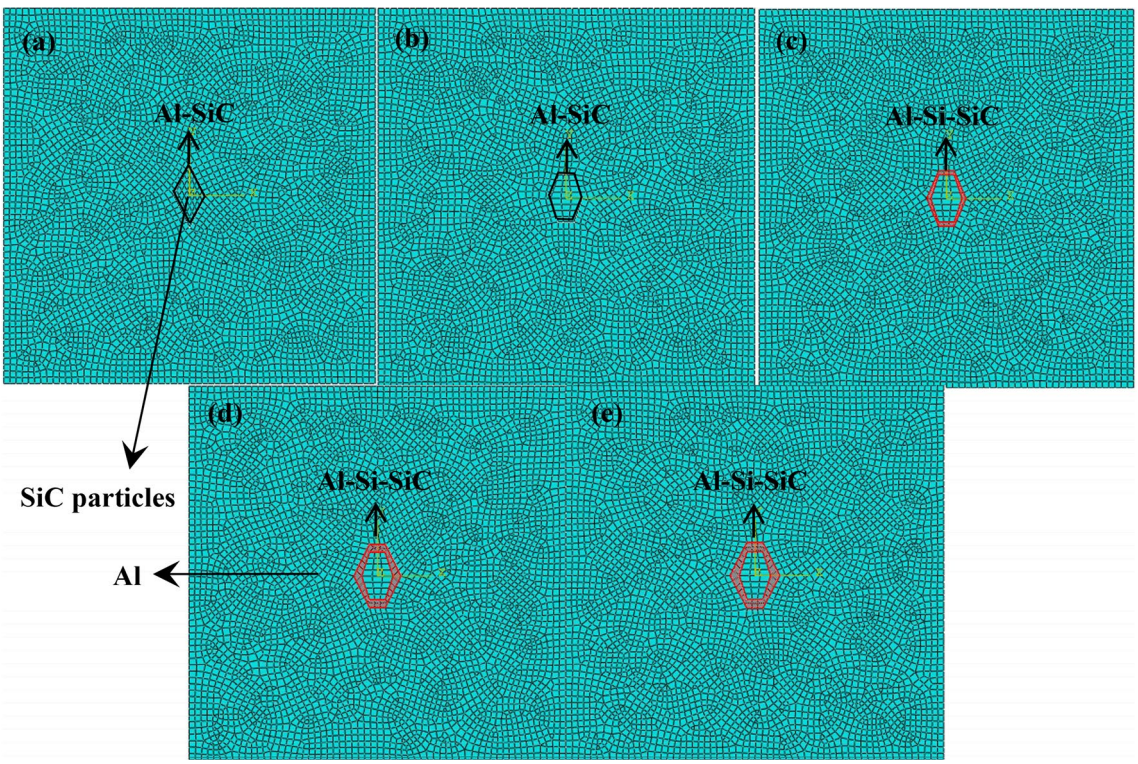

Fig. 6 Interface-phase model under different surface modification methods: **a** SiC particles A; **b** SiC particles B; **c** SiC particles C; **d** SiC particles D; **e** SiC particles E

Table 3 Physical properties of each component of SiCp/6061Al composites [26, 27]

Properties	Unit	Reinforcement	Matrix	Interphase (Si)
Density	g/cm3	3.13	2.7	2.33
Thermal conductivity	W/m K	81	180	150
Specific heat	J/kg K	427	880	703
Elastic modulus	Gpa	410	70.6	180
Poisson's ratio	–	0.14	0.34	0.28
Thermal expansion coefficient	10−6 K−1	4.9	23.6	2.5

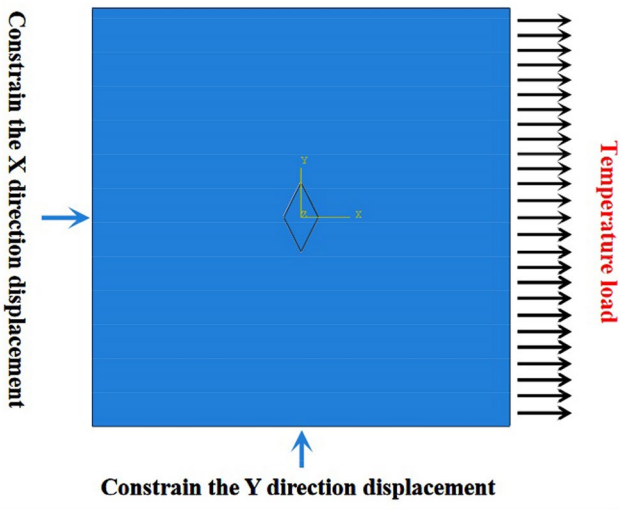

Fig. 7 The boundary conditions and temperature loads imposed on the interface-phase model

so that the displacement changes of nodes on the plane were subject to corresponding constraints. In this paper, the boundary conditions and temperature loads imposed on the interface-phase model are shown in Fig. 7.

3.5.3 Distribution of residual stress

Operate according to the set finite element simulation steps, after the loading calculation, the generated stress nephogram is shown in Fig. 8.

In Fig. 8a, it can be clearly seen that the RS is mainly distributed in the sharp corner region of reinforcement, and the stress level is relatively high. In Fig. 8b, the sharp corners of reinforcement are broken, and the RS is mainly distributed inside the reinforcement, but the overall stress level has decreased. This shows that eliminating the sharp corners of SiC particles can slow down the high concentration of RS. In Fig. 8c, the RS is mainly distributed in the

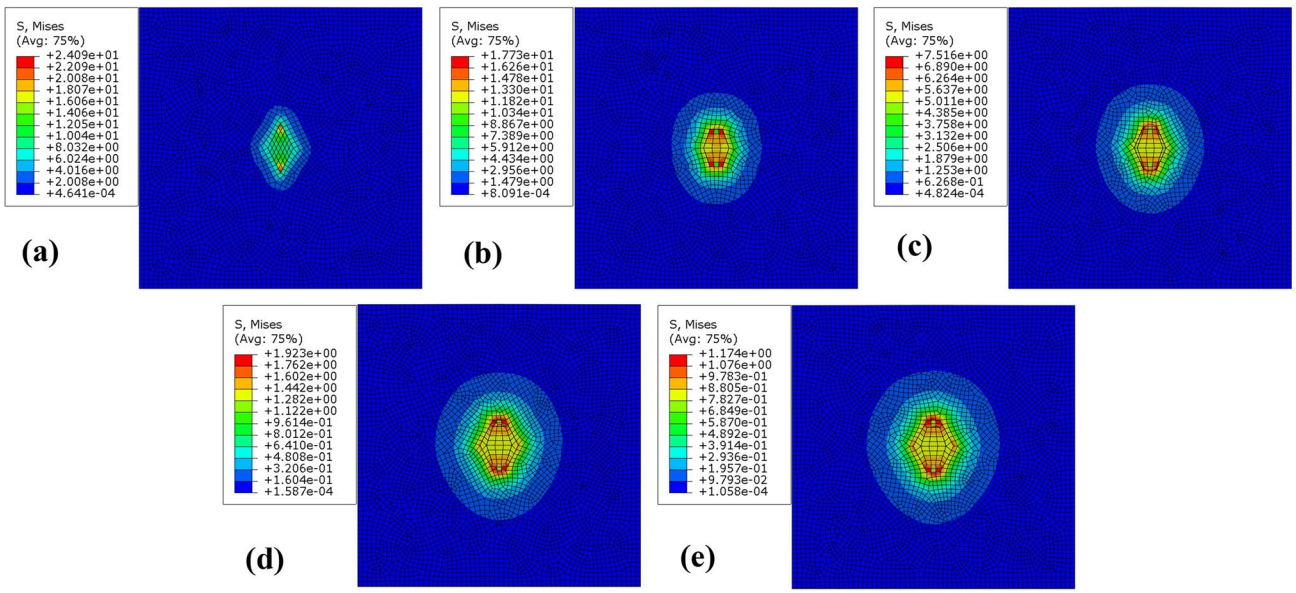

Fig. 8 Von Mises stress distribution under different surface modification methods: **a** SiC particles A; **b** SiC particles B; **c** SiC particles C; **d** SiC particles D; **e** SiC particles E

Al-Si-SiC interphase and reinforcement, and the stress level has decreased significantly. This is because the formation of Al-Si-SiC interphase inhibits the excessive erosion of matrix to the reinforcement and reduces the degree of interfacial reaction. In addition, the low coefficient of thermal expansion and elastic modulus of Si element are also one of the important factors that cause the stress level to decline. As the thickness of Al-Si-SiC interphase increases, the distribution of RS has not changed significantly, but the stress level is gradually decreasing. And after the thickness is increased to a certain extent, the RS level in SiCp/6061Al composites has a relatively decrease amplitude, as shown in Fig. 8d and e.

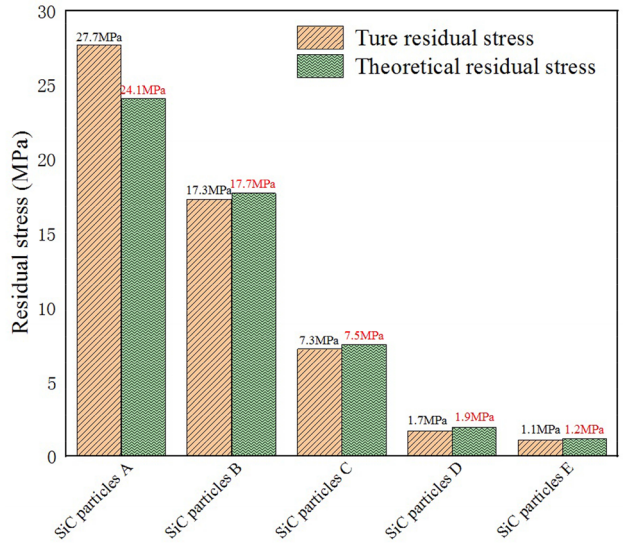

Fig. 9 Comparison of experimental measurement and finite element simulation results

According to the results reflected in Fig. 9, both experimental measurements and finite element simulations have confirmed that the reinforcement surface modification can effectively reduce the RS in SiCp/6061Al composites. Compared with pickling and ultrasonic stirring, high-temperature oxidation has a relatively higher degree of influence on the RS. With the extension of high-temperature oxidation time, the thickness of Al-Si-SiC interphase gradually increases, and its blocking effect is fully exerted, further reducing the RS in SiCp/6061Al composites.

3.6 Relaxation mechanism of residual stress

From the content shown in Fig. 10, in the process of surface modification, the sharp corners of SiC particles are gradually passivated, impurities such as Fe_2O_3 and C are completely removed, and a SiO_2 layer is formed on the surface of SiC particles. When preparing 35vo l%SiCp/6061Al composites, the SiO_2 layer and the molten aluminum alloy react chemically in a high-temperature environment, and the generated Si element is enriched in the interface region. Energy Dispersive Spectroscopy (EDS) is used to conduct elemental analysis on the experimental samples after surface modification, the presence of Si elements is detected in the interface region, and the proportion of Si atoms reached 93.81%. Meanwhile, it can also be clearly seen in the picture that the reinforcement and matrix are also in a tightly bonded state, which indicates that the enrichment of Si element contributes to the improvement of interface bonding strength.

In order to further verify the positive effect of Si element enrichment on the interface bonding strength, an atomic structure model of Al-Si-SiC interphase was constructed in this paper, and the interface adhesion work of Al-SiC and

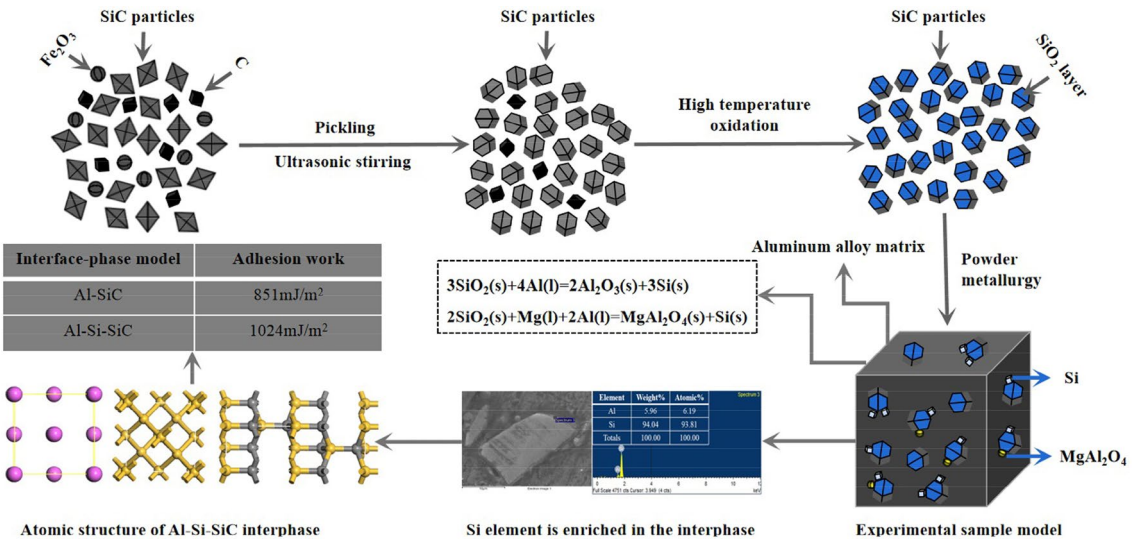

Fig. 10 The mechanism of reinforcement surface modification on interface bonding strength

Al-Si-SiC was preliminarily calculated based on the first principle [30]:

$$W_{ad} = \frac{E_{Al} + E_{SiC} - E_{Al-SiC}}{S} \quad (7)$$

In Eq. (7), E_{Al}, E_{SiC} and $E_{Al\text{-}SiC}$, respectively, represent the surface energy of matrix, reinforcement and interphase, and S represents the area of interphase. Combined with relevant data [31], the calculated interface adhesion work is shown in Fig. 10. Obviously, when Si atoms are doped into the atomic structure model of interphase, the interface adhesion work of SiCp/6061Al composites is significantly improved, and the corresponding interface bonding strength also increases.

According to the above analysis, pickling, ultrasonic stirring and high-temperature oxidation (1100 ℃/6 h) with SiC particles can prompt Si element enrichment in the interface region, forming Al-Si-SiC interphase, which significantly enhances the interface bonding strength of SiCp/6061Al composites. And the blocking effect of the Al-Si-SiC interphase can play a role in inhibiting crack propagation and slowing down the concentration degree of RS. Meanwhile, the elastic modulus of SiC particles is much higher than that of Si element, and its Poisson's ratio is lower than that of Si element. Combining Eq. 4, it can be clearly seen that the enrichment of Si element reduces the stress coefficient K of SiCp/6061Al composites.

4 Conclusion

In this paper, a combination of experimental analysis and numerical simulation was used to study the effect of reinforcement surface modification on the RS in SiCp/6061Al composites, and the following important conclusions were obtained.

After pickling, ultrasonic stirring and high-temperature oxidation (1100 ℃/6 h), the RS in 35vo l%SiCp/6061Al composites measured by X-ray diffraction method was 1.1 MPa.

The SiO_2 layer preferentially contacts the molten aluminum alloy and chemically reacts to form an Al-Si-SiC interphase, which significantly improved the interface bonding strength of SiCp/6061Al composites and promoted the concentration degree of RS to be slowed down.

An interface-phase model based on the surface morphology of real SiC particles was established. The simulation results show that the RS is mainly concentrated in the sharp corners of reinforcement, and the stress level is relatively high. When the sharp corners are eliminated, the stress level gradually decreases. When the Al-Si-SiC interphase is formed, the stress level in SiCp/6061Al composites decreases significantly. The results of finite element simulation and experimental measurement are relatively consistent.

Acknowledgement This work was financially supported by National Natural Science Foundation of China (Grant No. 52071002) and Anhui Province Postdoctoral Science Foundation (Grant No. 2017B213).

Declaration

Conflict of interest There are no conficts to declare.

Data availability statement Some or all data generated or used during the study are available from the corresponding author by request.

References

1. F. Qiu, X. Gao, J. Tang, Y.Y. Gao, S.L. Shu, X. Han, Q. Li, Q.C. Jiang, Microstructures and tensile properties of Al–Cu matrix composites reinforced with nano-sized SiCp fabricated by semi-solid stirring process. Metals **34**, 1–8 (2017)
2. S.B. Ren, X.H. Xu, J. Guo, X.B. He, M.L. Qin, X.Y. Shen, Net-shape forming and properties of high volume fraction SiCp/Al composites. J. Alloy. Compd. **484**, 256–262 (2009)
3. P.B. Li, T.J. Chen, H. Qin, Effects of pressure on microstructure and mechanical properties of SiCp/2024 Al-based composites fabricated by powder thixoforming. J. Mater. Sci. **52**, 2045–2059 (2017)
4. G. Meijer, F. Ellyin, Z. Xia, Aspects of residual thermal stress/strain in particle reinforced metal matrix composites. Compos. B. **31**, 29–37 (2000)
5. S. Chatterjee, S.G. Sur, S. Bandyopadhyay, A. Basumallick, Effect of microstructure and residual stresses on nano-tribological and tensile properties of Al_2O_3-and SiC-reinforced 6061-Al metal matrix composites. J. Compos. Mater. **50**, 2687–2698 (2016)
6. S.G. Qu, H.S. Lou, X.Q. Li, T.R. Kuang, J.Y. Lou, Effect of heat-treatment on stress relief and dimensional stability behavior of SiCp/Al composite with high SiC content. Mater. Des. **86**, 508–515 (2015)
7. X.J. Kong, M.H. Wang, B. Wang, Y.H. Zheng, L.J. Yang, Thermal mismatch stress relaxation and dislocation transformation of 45%SiCp/Al composites by continuous diode laser heating. Appl. Phys. A. **125**, 596–606 (2019)
8. G.Q. Wu, Q.Q. Zhang, X. Yang, Z. Huang, W. Sha, Effects of particle/matrix interface and strengthening mechanisms on the mechanical properties of metal matrix composites. Compos. Interfaces **21**, 415–429 (2014)
9. D.M. Jarząbek, The impact of weak interfacial bonding strength on mechanical properties of metal matrix-ceramic reinforced composites. Compos. Struct. **201**, 352–362 (2018)
10. R.M. Wang, M.K. Surappa, C.H. Tao, C.Z. Li, M.G. Yan, Microstructure and interface structure studies of SiCp-reinforced Al (6061) metal-matrix composites. Mater. Sci. Eng. A. **254**, 219–226 (1998)
11. B. Inem, G. Pollard, Interface structure and fractography of a magnesium-alloy, metal-matrix composite reinforced with SiC particles. J. Mater. Sci. **28**, 4427–4434 (1993)
12. Y.Y. Gao, F. Qiu, R. Geng, W.X. Zhao, D.L. Yang, R. Zuo, B.X. Dong, X. Han, Q.C. Jiang, Preparation and characterization of the Al-Cu-Mg-Si-Mn composites reinforced by different surface modified SiCp. Mater. Charact. **141**, 156–162 (2018)
13. G.W. Liu, W.Q. Luo, X.Z. Zhang, H.C. Shao, T.Z. Pan, Q.J. Qiao, Microstructure, mechanical and thermal properties of Ni-P(-SiC)

coating on high volume fraction SiCp/Al composite. Rare Met. **12**, 63–69 (2017)
14. P. Wang, Z. Gao, D.F. Cheng, D.X. Xu, J.T. Niu, Effect of Ni-P alloy coating on microstructures and properties of vacuum brazed joints of SiCp/Al composites. Mod. Phys. Lett. B. **31**, 1750082 (2017)
15. Z.L. Ni, A.Q. Wang, J.P. Xie, M. Fang, Influence of SiCp surface treatment on the SiCp/Al-30Si microstructure and performance. Adv. Mater. Res. **538–541**, 326–330 (2012)
16. J. Park, J. Lee, I. Jo, S. Cho, S.K. Lee, S.B. Lee, H.J. Ryu, S.H. Hong, Surface modification effects of SiC tile on the wettability and interfacial bond strength of SiC tile/Al7075-SiCp hybrid composites. Surf. Coat. Tech. **307**, 399–406 (2016)
17. V. Laurent, D. Chatain, N. Eustathopoulos, Wettability of SiO_2 and oxidized SiC by aluminium. Mater. Sci. Eng. A. **135**, 89–94 (1991)
18. A.H. Zou, X.L. Zhou, D.S. Li, Y.W. Yu, The influence of SiCp oxidized on the interface layer and thermal conductivity of SiCp/Al composites. Compos. Interfaces **20**, 107–117 (2013)
19. O. El-Kady, A. Fathy, Effect of SiC particle size on the physical and mechanical properties of extruded Al matrix nanocomposites. Mater. Des. **54**, 348–353 (2014)
20. D.L. Yang, F. Qiu, Q.L. Zhao, Q.C. Jiang, The microstructure and tensile property for Al2014 composites reinforced with Ti_5Si_3-coated SiCp. Mater. Sci. Eng. A. **688**, 459–463 (2017)
21. D.L. Yang, F. Qiu, W.X. Zhao, P. Shen, H.Y. Wang, Q.C. Jiang, Effects of Ti-coating layer on the distribution of SiCp in the SiCp/2014Al composites. Mater. Des. **87**, 1100–1106 (2015)
22. A. Pramanik, L.C. Zhang, J.A. Arsecularatne, Machining of metal matrix composites: Effect of ceramic particles on residual stress, surface roughness and chip formation. Int J Mach Tool Manu **48**, 1613–1625 (2008)
23. S. Bajpai, R. Kundu, K. Balani, Effect of B4C reinforcement on microstructure, residual stress, toughening and scratch resistance of (Hf, Zr)B2 ceramics. Mater. Sci. Eng. A. **796**, 140022 (2020)
24. J.C. Lee, H.I. Lee, J.P. Ahn, Z.L. Shi, Y.M. Kim, Modification of the interface in SiC/Al composites. Metall. Mater. Trans. A. **31**, 2361–2368 (2000)
25. Y. Lu, L. Hao, F.S. Pan, J.X. Chen, M. Hirohashi, A study of the residual stress and its influence on tensile behaviors of fiber-reinforced SiC/Al composite. Adv. Compos. Mater. **22**, 255–263 (2013)
26. Y.F. Wang, W.H. Liao, K. Yang, X.Y. Teng, W.Q. Chen, Simulation and experimental investigation on the cutting mechanism and surface generation in machining SiCp/Al MMCs. Int. J. Adv. Manuf. Tech. **100**, 1393–1404 (2019)
27. L. Zhou, C. Cui, P.F. Zhang, Z.Y. Ma, Finite element and experimental analysis of machinability during machining of high-volume fraction SiCp/Al composites. Int. J. Adv. Manuf. Tech. **91**, 1935–1944 (2017)
28. Q. Wang, R.L. Hou, J.X. Li, Y.L. Ke, Analytical and experimental study on deformation of thin-walled panel with non-ideal boundary conditions. Int. J. Mech. Sci. **149**, 298–310 (2018)
29. M.N. Yuan, Y.Q. Yang, C. Li, P.Y. Heng, L.Z. Li, Numerical analysis of the stress-strain distributions in the particle reinforced metal matrix composite SiC/6064Al. Mater. Des. **38**, 1–6 (2012)
30. L.X. Shi, P. Shen, D. Zhang, Q.C. Jiang, Wetting and evaporation behaviors of molten Mg-Al alloy drops on partially oxidized α-SiC substrates. Mater. Chem. Phys. **130**, 1125–1133 (2011)
31. A.H. Zou, X.L. Zhou, Z.B. Kang, Y.H. Rao, K.Y. Wu, Alloy elements on SiC/Al interface: A first-principle and experimental study. J. Inorg. Mater. **34**, 1167–1174 (2019)

Publisher's Note Springer Nature remains neutral with regard to jurisdictional claims in published maps and institutional affiliations.